Available online at www.sciencedirect.com
ScienceDirect
Solar Energy 112 (2015) 282–289
SOLAR ENERGY
www.elsevier.com/locate/solener

Exergy analysis of a solar pond integrated with solar collector

Ismail Bozkurt [a,*], Mehmet Karakilcik [b]

[a] Department of Mechanical Engineering, Faculty of Engineering, University of Adiyaman, Adiyaman 02040, Turkey
[b] Department of Physics, Faculty of Sciences and Letters, University of Cukurova, Adana 01330, Turkey

Received 14 February 2014; received in revised form 20 October 2014; accepted 5 December 2014

Communicated by: Associate Editor Aliakbar Akbarzadeh

Abstract

In this paper we present the energetic and exergetic performance of a solar pond integrated with four flat plate solar collectors. The integrated solar pond system was built and tested at Cukurova University in Adana, Turkey. The solar pond consists of salty water zones to prevent convection heat losses from the heat storage zone (HSZ) of the solar pond. The temperature distributions of the solar pond and the inlet–outlet of the heat exchanger were measured by using thermocouples and a data acquisition device. An energy and exergy models were developed to study the energetic and exergetic performance of the integrated solar pond. The energy and exergy performances were compared for the each zone of the solar pond. The reference environment temperature in the exergy analysis was specified as the average representative temperature of each month of the year. The energetic and exergetic performances of the integrated solar pond for the heat storage zone were found to be maximum 32.55% and 28.69% in August, and to be minimum 9.48% and 5.51% in January, respectively.

Keywords: Solar energy; Integrated solar pond; Energetic and exergetic analyses

1. Introduction

Solar energy is considered a key source for the future, not only for Turkey, but also for all over the world. Therefore, the development and usage of solar energy systems are increasingly becoming vital for sustainable economic development (Cetin and Egrican, 2011). One of the useful solar energy systems is solar pond. Its main advantage is to prevent convection heat losses by dissolving salt into the bottom layer of this pond, making it too heavy to rise to the surface, even when hot (Dincer and Rosen, 2011).

Due to the high solar energy potential in Turkey, solar thermal applications are interesting options for the future energy demand. Therefore, solar thermal systems may be an important option for the supply of the energy demand. Experimental and theoretical temperature distributions, performance analysis of the inner zones and exergy analysis were investigated for different dimensions solar ponds by Karakilcik et al. (2006a,b); Karakilcik and Dincer (2008); Karakilcik et al. (2013a). Recently published studies provide detailed analysis and assessments of energy performance of solar pond (Kurt et al., 2006a; Kurt and Özkaymak, 2006b; Dah et al., 2010; Karim et al., 2010; Saleh et al., 2011; Karim et al., 2011; Sakhrieh and Al-Salaymeh, 2013; Bozkurt et al., 2014). Some experimental and theoretical studies were investigated about integrated solar pond with different applications (El-Sebaii, 2005; Velmurugan and Srithar, 2007; El-Sebaii et al., 2008; Akbarzadeh et al., 2009; Velmurugan et al., 2009; Singh et al., 2011). Integrating solar pond with collector system

* Corresponding author.
E-mail addresses: ismail_bozkurt44@yahoo.com (I. Bozkurt), kkilcik@cu.edu.tr (M. Karakilcik).

http://dx.doi.org/10.1016/j.solener.2014.12.009

Nomenclature

A	surface area (m^2)
C	specific heat (J/kg K)
E	the amount of solar energy reaching to the pond (MJ/m^2)
F	absorbed energy fraction at a region of δ-thickness
h	solar radiation ratio
HSZ	heat storage zone
k	thermal conductivity (W/m °C)
m	mass (kg)
NCZ	non-convective zone
Q	heat (J)
s	salinity (g/kg)
T	temperature (K)
UCZ	upper convective zone
Greek Letters	
η	energy efficiency
Ξ	exergy (J)
δ	thickness where long wave solar energy is absorbed (m)
α	emissivity of the absorber surface of the flat plate collector
β	incident beam entering rate into water
θ	angle (rad)
ρ	density (kg/m^3)
T	transmission coefficient of the collector surface
ψ	exergy efficiency
Subscripts	
dest	destruction
dw	down wall
fpc	flat plate collector
i	incident
in	energy input
m	mean
out	energy output
r	refraction
solar	solar energy
st	heat stored inner zones of the pond
sw	side wall
up	just above zone

was studied to increase solar pond performance by Bozkurt and Karakilcik (2012). There are very little experimental and theoretical investigations on exergetic performance analysis of the solar ponds through exergy efficiency. The investigation of exergetic performance analysis of the solar pond and comparison with the corresponding energy efficiencies during the months of the year becomes the first work in this area (Karakilcik and Dincer, 2008). Furthermore, the dynamic exergetic performance assessment, through exergy efficiency of the integrated solar pond was studied according to the number of collectors by Karakilcik et al. (2013b).

The objective of the paper is to point out the energetic and exergetic performance assessment on the integrated solar pond during the year. For the experimental study, an integrated solar pond was constructed at Cukurova University in Adana, Turkey (i.e., 35°18′ E longitude, 37°05′ N latitude). The energetic and exergetic performance of the solar pond was increased by using four flat plate solar collectors. The heat energy which was obtained from four flat plate solar collectors was transferred to the heat storage zone of the solar pond by using a heat exchanger system. The energetic and exergetic performance of the integrated solar pond were determined and compared.

2. Integrated solar pond system

There are some differences between an ordinary pond or lake and a salt gradient solar pond. When solar energy is absorbed by an ordinary pond, water in the lower parts of the pond becomes warmer and rises to the surface of the pond, where it loses the absorbed heat to the ambient. In solar ponds, this phenomenon is inhibited by dissolving salt into lower parts of pond, making them heavier and keeps them from rising to the surface, even when the bottom water layer is hot (Dehghan et al., 2013). The integrated solar pond consists of a solar pond and four flat plate solar collectors. There are three zones in the solar pond. The bottom of the solar pond is filled with saturated salty water. This zone is called as Heat Storage Zone (HSZ). Afterward, the salty water layers whose brine density gradually decreases towards Upper Convective Zone (UCZ) are formed. This zone is called as Non-Convective Zone (NCZ). NCZ consists of four different density layers. NCZ is a transparent insulation zone to allow an extensive amount of solar radiation to penetrate into the storage zone while inhibiting the propagation of long-wave solar radiation from escaping because water is opaque to infrared radiation. Then the last zone UCZ is created with fresh water at the top of the pond. This zone provides the cleanliness of the pond and filling the lost water due to evaporation.

For the experimental study, an integrated solar pond consisting of the cylindrical solar pond, heat exchanger and four solar collectors were constructed as seen in Fig. 1. The solar pond has a radius of 0.80 m and a depth of 2 m. The conventional flat plate solar collector has dimensions of 1.90 m × 0.90 m. The thicknesses of the zones are 0.2, 0.8, 1 m for UCZ, NCZ and HSZ, respectively. The range of density is 1000–1030 kg/m^3 in UCZ,

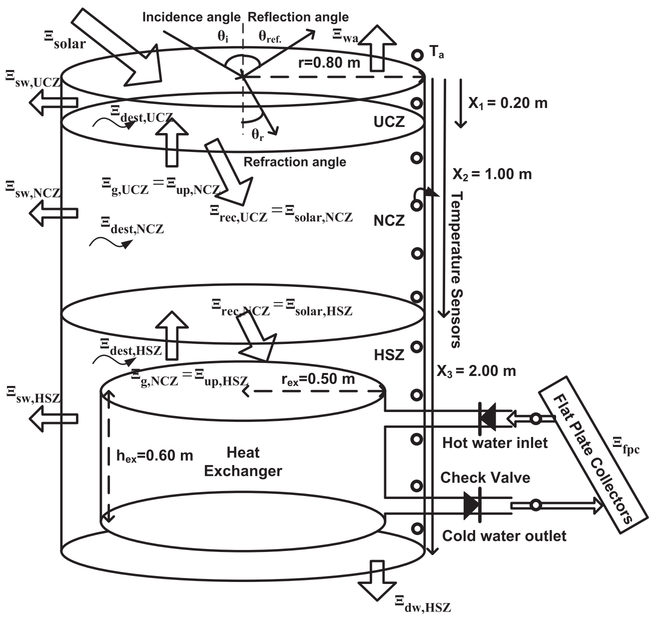

Fig. 1. Exergy fluxes of a solar pond system integrated with collectors.

1030–1165 kg/m^3 in NCZ and 1165–1185 kg/m^3 in HSZ. NCZ acts as a thermal and mass insulator for the lower layer. Its stability was investigated by Karim et al. (2010, 2011). To determine the temperature distribution of the inner zones and the inlet–outlet of the exchanger system, *J* type thermocouples were used. The thermocouples were placed into the inner zones, starting from the bottom, at 0.10, 0.30, 0.50, 0.70, 0.90, 1.10, 1.30, 1.50, 1.70, 1.90 m heights. Hence, the temperature distributions were obtained experimentally. The density distributions were measured by using hydrometer. To measure the density, the slim hoses were placed into the solar pond. The conventional four flat plate solar collectors were connected to the exchanger system to transfer heat energy from the collectors to HSZ with natural convection.

3. Energy and exergy analysis

An understanding of the difference between energetic and exergetic efficiency is the key role to reveal the real performance of the energy systems. Energy cannot be created or destroyed but not exergy. It can be degraded in quality, eventually reaching a state in which it is in completed equilibrium with the dead state. It appears to be a potential tool for design, analysis, evaluation, and performance improvement of solar pond systems (Dincer and Rosen, 2011). All temperature measurements were taken as °C, however they were converted to thermodynamic temperature scale (K) for the energy and exergy calculations.

In this study, the made assumptions are listed below:

- The temperature dependence of the heat capacity was neglected.
- The monthly average density and heat capacity were used for inner zones.
- The heat transfer coefficients of the materials were considered constant.
- All calculations for the energy and exergy values were done hourly basis.
- The convection and radiation heat loss in the solar pond were neglected.

3.1. Energy and exergy analysis for HSZ

The performance of the solar pond system integrated with collectors will be evaluated with the energy and exergy analysis methods. The mass, energy and exergy balances of the integrated solar pond are established. The mass balance is given by:

$$\sum_t \dot{m}_{\mathrm{in}} = \sum_t \dot{m}_{\mathrm{out}} \tag{1}$$

where $\dot{m}_{\mathrm{in}}$ and $\dot{m}_{\mathrm{out}}$ stand for the inlet and outlet flows of the heat exchanger. The energy balance of HSZ is given by:

$$\sum_t \dot{\mathrm{Q}}_{\mathrm{st}} = \sum_t \dot{\mathrm{Q}}_{\mathrm{in}} - \sum_t \dot{\mathrm{Q}}_{\mathrm{out}} = \sum_t (\dot{\mathrm{Q}}_{\mathrm{solar,HSZ}} + \dot{\mathrm{Q}}_{\mathrm{fpc}}) - \sum_t (\dot{\mathrm{Q}}_{\mathrm{up,HSZ}} + \dot{\mathrm{Q}}_{\mathrm{dw,HSZ}} + \dot{\mathrm{Q}}_{\mathrm{sw,HSZ}}) \tag{2}$$

where $\dot{\mathrm{Q}}_{\mathrm{st}}$ is the stored heat energy rate in HSZ, $\dot{\mathrm{Q}}_{\mathrm{in}}$ is the total input heat energy rate of HSZ, $\dot{\mathrm{Q}}_{\mathrm{out}}$ is the total output heat energy rate of HSZ, $\dot{\mathrm{Q}}_{\mathrm{solar,HSZ}}$ is the amount of solar energy rate reaching HSZ, $\dot{\mathrm{Q}}_{\mathrm{fpc}}$ is the amount of solar energy rate reaching the flat plate collectors, $\dot{\mathrm{Q}}_{\mathrm{dw,HSZ}}$ is the total heat loss rate to the down wall from HSZ, $\dot{\mathrm{Q}}_{\mathrm{up,HSZ}}$ is the heat loss rate from HSZ to NCZ, $\dot{\mathrm{Q}}_{\mathrm{sw,HSZ}}$ is the total heat loss rate to the side wall of HSZ.

The energy efficiency of heat storage zone is given by:

$$\eta = \frac{\sum_t \dot{\mathrm{Q}}_{\mathrm{st}}}{\sum_t \dot{\mathrm{Q}}_{\mathrm{in}}} == \frac{\sum_t m_{\mathrm{HSZ}} \mathrm{C}_{\mathrm{p,HSZ}} (T_{\mathrm{HSZ,final}} - T_{\mathrm{HSZ,initial}})}{\sum_t (\beta \dot{\mathrm{E}} \mathrm{A}[(1-\mathrm{F})\mathrm{h}(\mathrm{x}_3 - \delta)] + \dot{\mathrm{E}}(\tau\alpha)\mathrm{A}_{\mathrm{fpc}})} \tag{3}$$

The fraction of the incident solar radiation that enters the pond is written by using an expression (Hawlader, 1980):

$$\beta = 1 - 0.6 \left[\frac{\sin\theta_i - \sin\theta_r}{\sin\theta_i + \sin\theta_r}\right]^2 - 0.4 \left[\frac{\tan\theta_i - \tan\theta_r}{\tan\theta_i + \tan\theta_r}\right]^2 \tag{4}$$

where θ_i and θ_r are the angles of incidence and refraction.

The ratio of the amount of solar energy reaching in the pond (h) is given (Bryant and Colbec, 1977) as:

$$\mathrm{h} = 0.727 - 0.056 \ln\left[\frac{(\mathrm{x} - \delta)}{cos\theta_{\mathrm{r}}}\right] \tag{5}$$

Here we present a comprehensive exergy analysis of integrated solar pond. The exergy flows are well outlined in Fig. 1. The exergy of solar radiation can be expressed by as modified from Petela (Petala, 2003):

$$\sum_t \dot{\Xi}_{solar} = \sum_t \dot{E}_{net}\left[1 - \frac{4T_0}{3T} + \frac{1}{3}\left(\frac{T_0}{T}\right)^4\right] \tag{6}$$

where $\dot{E}_{net}$ is the net incident solar radiation ratio reaching the surface, ψT is the sun's surface temperature, T_0 is the reference temperature. The exergy flows in HSZ are clearly shown in Fig. 1 and the stored exergy equation in this regard results in:

$$\sum_t \dot{\Xi}_{st} = \sum_t (\dot{\Xi}_{solar,HSZ} + \dot{\Xi}_{fpc}) - \sum_t (\dot{\Xi}_{up,HSZ} + \dot{\Xi}_{sw,HSZ} + \dot{\Xi}_{dw,HSZ} + \dot{\Xi}_{dest,HSZ}) \tag{7}$$

where $\dot{\Xi}_{st}$ is the stored exergy rate in HSZ, $\dot{\Xi}_{solar,HSZ}$ is the amount of solar exergy rate reaching from NCZ to HSZ, $\dot{\Xi}_{fpc}$ is the gained exergy rate from the solar collectors, $\dot{\Xi}_{up,HSZ}$ is the exergy loss rate from HSZ to NCZ, $\dot{\Xi}_{sw,HSZ}$ is the exergy loss rate through side wall, $\dot{\Xi}_{dw,HSZ}$ the exergy loss rate through down wall, $\dot{\Xi}_{dest,HSZ}$ the exergy destruction in HSZ. We can now define the exergy efficiency for HSZ as the ratio of the exergy stored in HSZ to the total exergy input to HSZ:

$$\psi = \frac{\sum_t \dot{\Xi}_{st}}{\sum_t \dot{\Xi}_{in}} = \frac{\sum_t m_{HSZ} C_{p,HSZ}[(T_{HSZ,final} - T_{HSZ,initial}) - T_o \ln(T_{HSZ,final}/T_{HSZ,initial})]}{\sum_t (\beta \dot{\Xi}_{solar} A[(1 - F)h(x_3 - \delta)] + \dot{\Xi}_{solar}(\tau\alpha)A_{fpc})} \tag{8}$$

3.1. Energy and exergy analysis for NCZ

The energy balance of NCZ is written as:

$$\sum_t \dot{Q}_{st} = \sum_t \dot{Q}_{in} - \sum_t \dot{Q}_{out} = \sum_t (\dot{Q}_{solar,NCZ} + \dot{Q}_{up,HSZ}) - \sum_t (\dot{Q}_{up,NCZ} + \dot{Q}_{sw,NCZ}) \tag{9}$$

The energy efficiency of NCZ is given by:

$$\eta = \frac{\sum_t \dot{Q}_{st}}{\sum_t \dot{Q}_{in}} = \frac{\sum_t m_{NCZ} C_{p,NCZ}(T_{NCZ,final} - T_{NCZ,initial})}{\sum_t (\beta \dot{E} A[(1 - F)h(x_2 - \delta)] + \frac{k_{salt,w} A}{\Delta x_{HSZ-NCZ}}(T_{m,HSZ} - T_{m,NCZ})} \tag{10}$$

The exergy flows in NCZ are clearly shown in Fig. 1 and the stored exergy equation in this regard results in:

$$\sum_t \dot{\Xi}_{st} = \sum_t (\dot{\Xi}_{solar,NCZ} + \dot{\Xi}_{up,HSZ}) - \sum_t (\dot{\Xi}_{up,NCZ} + \dot{\Xi}_{sw,NCZ} + \dot{\Xi}_{dest,NCZ}) \tag{11}$$

We can now write the exergy efficiency for the NCZ as:

$$\psi = \frac{\sum_t \dot{\Xi}_{st}}{\sum_t \dot{\Xi}_{in}} = \frac{\sum_t m_{NCZ} C_{p,NCZ}[(T_{NCZ,final} - T_{NCZ,initial}) - T_o \ln(T_{NCZ,final}/T_{NCZ,initial})]}{\sum_t (\beta \dot{\Xi}_{solar} A[(1 - F)h(x_2 - \delta)] + m_{HSZ} C_{p,HSZ}\left[(T_{m,HSZ} - T_{m,NCZ}) - T_0\left(\ln \frac{T_{m,HSZ}}{T_{m,NCZ}}\right)\right]} \tag{12}$$

3.2. Energy and Exergy Analysis for UCZ

The energy balance of UCZ is written as:

$$\sum_t \dot{Q}_{st} = \sum_t \dot{Q}_{in} - \sum_t \dot{Q}_{out} = \sum_t (\dot{Q}_{solar,UCZ} + \dot{Q}_{up,NCZ}) - \sum_t (\dot{Q}_{up,UCZ} + \dot{Q}_{sw,UCZ}) \tag{13}$$

The energy efficiency of UCZ is given by:

$$\eta = \frac{\sum_t \dot{Q}_{st}}{\sum_t \dot{Q}_{in}} = \frac{\sum_t m_{UCZ} C_{p,UCZ}(T_{UCZ,final} - T_{UCZ,initial})}{\sum_t (\beta \dot{E} A[(1 - F)h(x_1 - \delta)] + \frac{k_{salt,w} A}{\Delta x_{NCZ-UCZ}}(T_{m,NCZ} - T_{m,UCZ})} \tag{14}$$

The exergy flows in UCZ are clearly shown in Fig. 1 and the stored exergy equation in this regard results in:

$$\sum_t \dot{\Xi}_{st} = \sum_t (\dot{\Xi}_{solar,UCZ} + \dot{\Xi}_{up,NCZ}) - \sum_t (\dot{\Xi}_{up,UCZ} + \dot{\Xi}_{sw,UCZ} + \dot{\Xi}_{dest,UCZ}) \quad (15)$$

We can now write the exergy efficiency for the UCZ as:

$$\psi = \frac{\sum_t \dot{\Xi}_{st}}{\sum_t \dot{\Xi}_{in}} = \frac{\sum_t m_{UCZ} C_{p,UCZ} [(T_{UCZ,final} - T_{UCZ,initial}) - T_o \ln(T_{UCZ,final}/T_{UCZ,initial})]}{\sum_t (\beta \dot{\Xi}_{solar} A[(1-F)h(x_1 - \delta)] + m_{NCZ} C_{p,NCZ} \left[(T_{m,NCZ} - T_{m,UCZ}) - T_0 \left(\ln \frac{T_{m,NCZ}}{T_{m,UCZ}}\right)\right]} \quad (16)$$

The specific heat capacity was determined by using an empirical equation (Sun et al., 2008):

$$C = (-0.0044s + 4.1569)1000 \quad (17)$$

where C is heat capacity, s is salinity. The density difference at low temperature takes place approximately in linear relationship between density and salinity. We used an empirical correlation as given below to determine the salinity of the zones (Sun et al., 2008):

$$s = \frac{(\rho - 998.24)}{0.756} \quad (18)$$

4. Results and discussion

In this work, we presented the results of the determination for both energy and exergy efficiencies for integrated solar pond during the year. The results were compared to determine true magnitudes of the losses taking place in the integrated system. The stability of salt density distribution is very important for solar pond. The density distribution of the integrated solar pond is shown in Fig. 2.

As seen in Fig. 2, the few changes were observed between the density variations during the year. The average density of HSZ and NCZ could be held stable. Thus, the salt gradient in the pond provided the prevention of the heat loss by convection. The density change of UCZ was prevented by adding fresh water instead of evaporating water. Table 1 lists the mass, volume and specific heat capacity of the zones. The mass was calculated by using volume and average density. The specific heat capacity was calculated by using density and salinity (by using Eq. (18)). The experimental temperature measurements were taken from integrated solar pond during the year. Experimental studies were performed using four collectors to increase the temperature of HSZ. Considering the energy efficiency with respect to surface area of the solar pond and the collectors, four solar collectors are suitable for using in this study. The temperature distribution of the integrated solar pond is shown in Fig. 3.

As seen in Fig. 3, the temperature of UCZ is observed to be a maximum of 35.0 °C in August, a minimum of 10.4 °C in January. Similarly, the temperature of NCZ is observed to be a maximum of 44.8 °C in August, a minimum of 13.9 °C in January, while the temperature of HSZ is observed to be a maximum of 55.20 °C in August, a minimum of 16.91 °C in January. The temperature distribution increases toward the bottom of the pond like the density distribution. The pond temperature began to rise rapidly in February. The temperature distribution of the exchanger and reference ambient temperatures were listed in Table 2. The experimental data of the integrated solar pond was subjected to the analysis of variance (one-way Anova) by

Table 1
The mass, volume and specific heat capacity of the zones.

	HSZ	NCZ	UCZ
Mass (kg)	2373.90	1746.30	408.01
Volume (m^3)	2.01	1.61	0.40
Specific heat capacity (J/kg °C)	3091.61	3644.83	4058.61

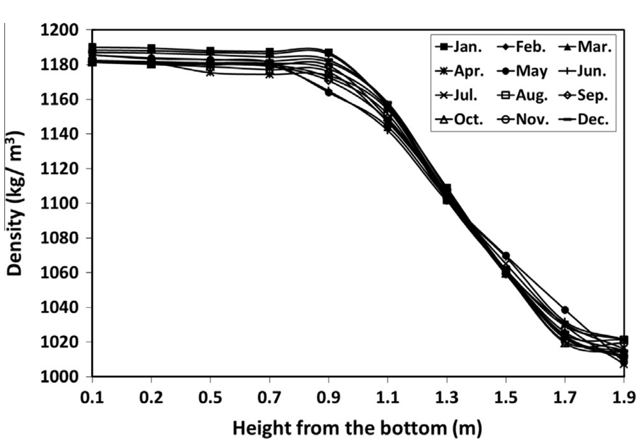

Fig. 2. The experimental density distribution of the integrated solar pond.

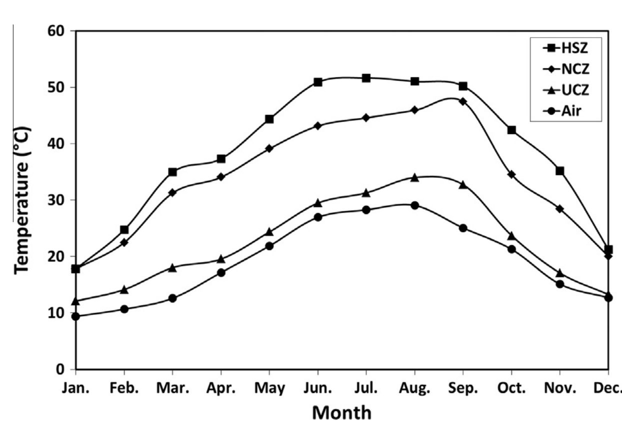

Fig. 3. The temperature distribution of the integrated solar pond.

Table 2
Average temperature distribution of the exchanger and reference ambient temperatures.

Month	Inlet (°C)	Outlet (°C)	Ref. Temp. (°C)
January	22.3	11.8	9.4
February	30.3	15.5	10.2
March	39.9	20.1	12.6
April	41.5	25.7	17.2
May	49.8	30.5	21.9
June	54.4	36.0	27.0
July	54.9	38.6	28.3
August	54.1	38.5	29.0
September	51.7	37.8	25.1
October	50.6	30.2	21.3
November	47.3	27.4	15.1
December	24.5	15.0	12.7

Table 3
Proximate composition of the experimental temperature data during the year and zones with ±standard error for the integrated solar pond.

Month	HSZ $\overline{X} \pm SE$	NCZ $\overline{X} \pm SE$	UCZ $\overline{X} \pm SE$
January	17.79 ± 0.280h	17.30 ± 0.145k	12.10 ± 0.082l
February	24.75 ± 0.803f	22.49 ± 0.627i	14.14 ± 0.452j
March	34.93 ± 0.866e	31.27 ± 0.612g	18.03 ± 0.371h
April	37.34 ± 0.350d	34.06 ± 0.239f	19.55 ± 0.371g
May	44.38 ± 1.034c	39.10 ± 0.723e	24.36 ± 0.400e
June	50.89 ± 0.485a	43.15 ± 0.344d	29.47 ± 0.211d
July	51.65 ± 0.239a	44.59 ± 0.439c	31.30 ± 0.287c
August	51.03 ± 0.333a	45.91 ± 0.393b	34.00 ± 0.289a
September	50.20 ± 0.506a	47.42 ± 0.357a	32.73 ± 0.319b
October	42.44 ± 0.450c	34.51 ± 0.266f	21.70 ± 0.328f
November	35.17 ± 0.863e	28.39 ± 0.359h	16.06 ± 0.108i
December	21.22 ± 0.792g	20.04 ± 0.449j	13.25 ± 0.124k

using SPSS 15.0 (2006) and the Duncan's multiple range tests. These tests were performed to determine the significant differences between the means. Table 3 shows the proximate composition of the experimental temperature data during the year with ±standard errors.

The solar energy data were obtained from a local meteorological station. The exergy distribution was determined by using Eq. (6). Fig. 4 shows both average energy and

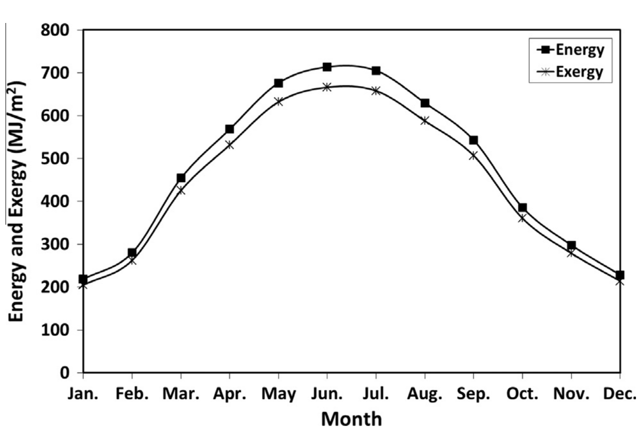

Fig. 4. Energy and exergy distributions of the solar energy in Adana, Turkey.

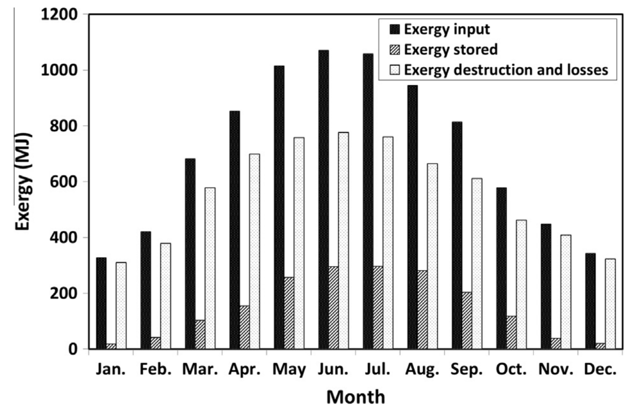

Fig. 5. Variations of the exergy input, stored, destruction and losses of HSZ.

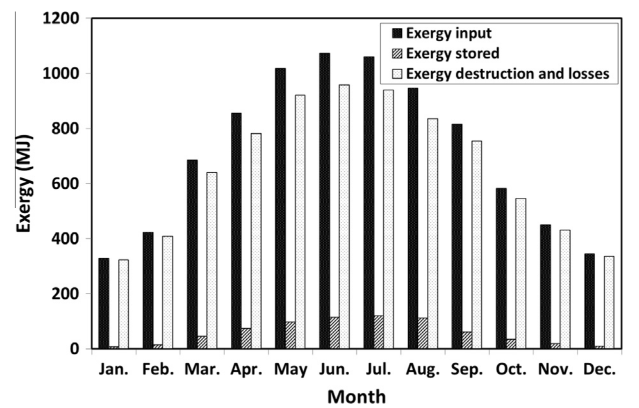

Fig. 6. Variations of the exergy input, stored, destruction and losses of NCZ.

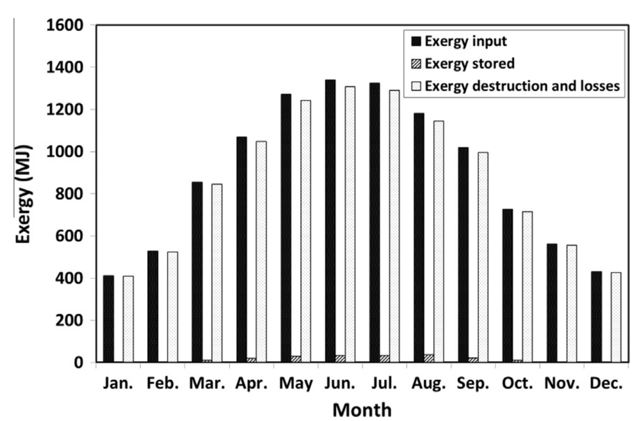

Fig. 7. Variations of the exergy input, stored, destruction and losses of UCZ.

exergy distribution during the year. The exergy contents are less than the corresponding energy contents due to the fact that energy is conserved, but not exergy. Thus, some exergy was lost to the surrounding and exergy destructed in the system. As seen in Fig. 4, the minimum energy and exergy content were observed as 218.48 MJ/m^2 and 204.77 MJ/m^2 in January, respectively. The maximum energy and exergy content were observed as

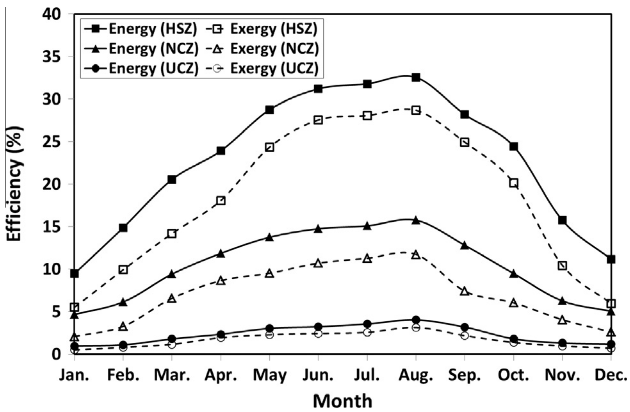

Fig. 8. Variations of the energy and exergy efficiencies of the integrated solar pond.

713.91 MJ/m^2 and 666.32 MJ/m^2 in June, respectively. It is understood that this region is quite rich in solar energy.

Figs. 5–7 show the variation of the exergy input, exergy stored, exergy destruction and losses for the zones of the solar pond during the year. The exergy content distributions were calculated by using the reference environment temperatures, average temperature distribution in the solar pond. As seen in Figs. 5–7, the stored exergy for HSZ, NCZ and UCZ appear to be maximum as 280.52 MJ, 111.08 MJ and 37.29 MJ in August, respectively. The stored exergy for HSZ, NCZ and UCZ appear to be minimum as 18.06 MJ, 6.78 MJ and 2.08 MJ in January, respectively. The stored energy in the HSZ and NCZ were calculated by using Eqs. (2) and (9). As a result, the energy stored in HSZ and NCZ appears to be maximum as 341.64 MJ and 185.53 MJ in August, to be minimum as 33.20 MJ and 16.41 MJ in January, respectively. It is understood that the significant amount of energy was stored in HSZ. However, an amount of energy was stored in NCZ. On the other hand, it seems that there is almost no energy was stored in UCZ because this zone is the surface of the solar pond.

The energetic and exergetic performance of the solar pond depends upon the total radiation reaching its surface and insulation. In this study, the glass wool was used for insulation, the flat plate collectors were used to increase surface area. Fig. 8 shows a comparison of both energy and exergy performances. The energy efficiencies for HSZ, NCZ and UCZ were found to be maximum as 33.55%, 15.75% and 4.04% in August, respectively. The solar pond exergy efficiencies for HSZ, NCZ and UCZ were found to be maximum as 28.69%, 11.74% and 3.15% in August, respectively. Furthermore, the solar pond energy efficiencies for HSZ, NCZ and UCZ were found to be minimum as 9.48%, 4.67% and 0.96% in January, respectively. The solar pond exergy efficiencies for HSZ, NCZ and UCZ were found to be minimum as 5.51%, 2.06% and 0.51% in January, respectively.

Bozkurt et al. (2014) investigated energy efficiency assessment of integrated and nonintegrated solar ponds (with and without the solar collectors). In the study, an experimental investigation of temperature distribution and efficiencies in conventional solar pond and integrated solar pond systems was presented. In addition, the monthly stored energies of solar pond and integrated solar pond were determined. The maximum and the minimum energy efficiencies of solar pond and integrated solar pond were observed for the months of August as 28.41% and 33.55% and January as 8.28% and 9.48%, respectively. In this way, the better energetic and exergetic performance of the solar pond were obtained.

The flat plate collectors have an important effect on energetic and exergetic performance of the solar pond. The more energy storage in solar pond was provided by using solar collectors by forming more surface area. To increase the energetic and exergetic performance of the solar pond, the exergy destruction and losses should be minimized.

5. Conclusions

This paper presents the results of energy and exergy analysis for an integrated solar pond. The energy and exergy efficiencies were calculated by using the experimental data for the integrated solar pond during the year. The use of exergy analysis in an integrated solar pond is very important to identify the sites of greatest losses and to improve the performance of the system. From this analysis, the exergetic efficiencies appear to be less than the energetic efficiencies for the integrated solar pond due to the exergy destructions in the zones and losses to the surroundings. As a results, the exergy efficiencies of HSZ, NCZ and UCZ for integrated system were found to be maximum as 28.69%, 11.74% and 3.15% in August, respectively. This study demonstrates that the exergy efficiency of the integrated solar pond is an important parameter in practical applications.

Acknowledgement

The authors are thankful to University of Cukurova in Turkey for financial support of the present work (Grant No: FEF2010BAP5).

References

Akbarzadeh, A., Johnson, P., Singh, R., 2009. Examining potential benefits of combining a chimney with a salinity gradient solar pond for production of power in salt affected areas. Sol. Energy 83, 1345–1359.

Bozkurt, I., Karakilcik, M., 2012. The daily performance of a solar pond integrated with solar collectors. Sol. Energy 86, 1611–1620.

Bozkurt, I., Atiz, A., Karakilcik, M., Dincer, I., 2014a. An investigation of the effect of transparent covers on the performance of cylindrical solar ponds. Int. J. Green Energy 11, 404–416.

Bozkurt, I., Karakilcik, M., Dincer, I., 2014b. Energy efficiency assessment of integrated and nonintegrated solar ponds. Int. J. Low-Carbon Technol. 9, 45–51.

Bryant, H.C., Colbec, I., 1977. A solar pond for London. Sol. Energy 19, 321–322.

Cetin, M., Egrican, N., 2011. Employment impacts of solar energy in Turkey. Energy Policy 39, 7184–7190.

Dehghan, A.A., Movahedi, A., Mazidi, M., 2013. Experimental investigation of energy and exergy performance of square and circular solar ponds. Sol. Energy 97, 273–284.
Dah, M.M.O., Ouni, M., Guizani, A., Belghith, A., 2010. The influence of the heat extraction mode on the performance and stability of a mini solar pond. Appl. Energy 87, 3005–3010.
Dincer, I., Rosen, M.A., 2011. Thermal Energy Storage Systems and Applications, second ed. Wiley, New York.
El-Sebaii, A.A., 2005. Thermal performance of a shallow solar-pond integrated with a baffle plate. Appl. Energy 81, 33–53.
El-Sebaii, A.A., Ramadan, M.R.I., Aboul-Enein, S., Salem, N., 2008. Thermal performance of a single-basin solar still integrated with a shallow solar pond. Energy Convers. Manage. 49, 2839–2848.
Hawlader, M.N.A., 1980. The influence of the extinction coefficient on the effectiveness of solar ponds. Sol. Energy 25, 461–464.
Karakilcik, M., Kıymac, K., Dincer, I., 2006a. Experimental and theoretical temperature distributions in a solar pond. Int. J. Heat Mass Transf. 49, 825–835.
Karakilcik, M., Dincer, I., Rosen, M.A., 2006b. Performance investigation of a solar pond. Appl. Therm. Eng. 26, 727–735.
Karakilcik, M., Dincer, I., 2008. Exergetic performance analysis of a solar pond. Int. J. Therm. Sci. 47, 93–102.
Karakilcik, M., Dincer, I., Bozkurt, I., Atiz, A., 2013a. Performance assessment of a solar pond with and without shading effect. Energy Convers. Manage. 65, 98–107.
Karakilcik, M., Bozkurt, I., Dincer, I., 2013b. Dynamic exergetic performance assessment of an integrated solar pond. Int. J. Exergy 12, 70–86.
Karim, C., Slim, Z., Kais, C., Jomaa, S.M., Akbarzadeh, A., 2010. Experimental study of the salt gradient solar pond stability. Sol. Energy 84, 24–31.
Karim, C., Jomaa, S.M., Akbarzadeh, A., 2011. A laboratory experimental study of mixing the solar pond gradient zone. Sol. Energy 85, 404–417.
Kurt, H., Ozkaymak, M., Binark, A.K., 2006a. Experimental and numerical analysis of sodium carbonate salt gradient solar pond performance under simulated solar radiation. Appl. Energy 83, 324–342.
Kurt, H., Özkaymak, M., 2006b. Performance evaluation of a small scale sodium carbonate salt gradient solar pond. Int. J. Energy Res. 30, 905–914.
Petala, R., 2003. Exergy of undiluted thermal radiations. Sol. Energy 74, 469–488.
Sakhrieh, A., Al-Salaymeh, A., 2013. Experimental and numerical investigations of salt gradient solar pond under Jordanian climate conditions. Energy Convers. Manage. 65, 725–728.
Saleh, A., Qudeiri, J.A., Al-Nimr, M.A., 2011. Performance investigation of a salt gradient solar pond coupled with desalination facility near the Dead Sea. Energy 36, 922–931.
Singh, R., Tundee, S., Akbarzadeh, A., 2011. Electric power generation from solar pond using combined thermosyphon and thermoelectric modules. Sol. Energy 85, 371–378.
SPSS, 2006. Computer program, MS for Windows, version 15.0, SPSS Inc., USA.
Sun, H., Feistel, R., Koch, M., Marko, A., 2008. New equations for density, entropy, heat capacity, and potential temperature of a saline thermal fluid. Deep Sea Res. Part I 55, 1304–1310.
Velmurugan, V., Srithar, K., 2007. Solar stills integrated with a mini solar pond-analytical simulation and experimental validation. Desalination 216, 232–241.
Velmurugan, V., Pandiarajan, S., Guruparan, P., Subramanian, L.H., Prabaharan, C.D., Srithar, K., 2009. Integrated performance of stepped and single basin solar stills with mini solar pond. Desalination 249, 902–909.